Supplementary information: Role of hydrogen bonding in the catalytic reduction of nitric oxide

Akitoshi Shiotari, Shinichiro Hatta, Hiroshi Okuyama, and Tetsuya Aruga
Department of Chemistry, Graduate School of Science, Kyoto University, Kyoto 606-8502, Japan

1 Formation process of a NO–OH complex

A OH (hydroxyl) group was produced by controlled dissociation of a water molecule by applying a voltage pulse of 2 V.[1] An OH group is imaged as a double depression, which results from dynamical flipping of the O–H bond between two equivalent orientations (Fig. S1c). Because the OH group cannot be manipulated to move across the surface, we manipulated a NO molecule to produce a NO–OH complex (Figs. S1a and S1b). The NO molecule can be translated along the Cu row in the "pulling" mode,[2] and encountered with a OH group located in the next row. Upon formation of the complex, the NO molecule is imaged as a "crescent" shape, indicating H-bond coupling, analogous to the case of NO-water interaction. The dynamical flip motion of OH group is probably frozen with the H-atom donated to the NO molecule (Fig. S1d).

2 Fitting $\mathrm{d}I/\mathrm{d}V$ curves of a $(OH)_2\cdots$NH–OH product

The dI/dV in Fig. 6e is analyzed by a recently proposed analytical modeling.[3,4] The product forms a chain of OH, OH, NH, and OH, as illustrated in Fig. S2c. Upon vibrational excitation by tunneling electrons, the two OH groups (OH dimer) is induced to flip between two different configurations (Figs. S2a and b), which causes the two-state fluctuation in the current. As a result, the dI/dV shows the characteristic peak-and-dip structure as a function of voltage, as shown in Fig. 6f.

Therefore, the tunneling current I depends on the applied bias V, the relative occupation $n_{H(L)}$ for the high (low) conductance states, and the corresponding conductance $\sigma_{H(L)}$ as,

$$I(V) = V[\sigma_L(V)n_L(V)+\sigma_H(V)n_H(V)], \tag{1}$$

where $n_{H(L)}$ is determined as a stationary solution of the rate equations,

$$\frac{\mathrm{d}n_H(V)}{\mathrm{d}t} = \Gamma^{L\to H}(V)\,n_L(V)-\Gamma^{H\to L}(V)\,n_H(V), \tag{2}$$

$$\frac{\mathrm{d}n_L(V)}{\mathrm{d}t} = \Gamma^{H\to L}(V)\,n_H(V)-\Gamma^{L\to H}(V)\,n_L(V), \tag{3}$$

with the condition $n_L + n_H = 1$. This gives

$$n_L(V) = \frac{\Gamma^{H\to L}(V)}{\Gamma^{H\to L}(V)+\Gamma^{L\to H}(V)}, \quad n_H(V) = \frac{\Gamma^{L\to H}(V)}{\Gamma^{H\to L}(V)+\Gamma^{L\to H}(V)}, \tag{4}$$

where $\Gamma^{H\to L(L\to H)}$ is the transition rate from the high- to low- (from the low- to high-) conductance configuration. The simplest way to model the transition rates is to assume a linear dependence on the vibrational generation rate, *i.e.*, in a single electron process,

$$\Gamma^{H\to L(L\to H)}(V) = \Gamma_0^{H(L)} + \sum_\nu C_\nu \Gamma_{\mathrm{em},\nu}^{H(L)}(V), \tag{5}$$

where a constant rate $\Gamma_0^{H(L)}$ is introduced to take into account the collective effect of many low-energy vibration modes mainly involving O atom motions, and where C_ν and $\Gamma_{\mathrm{em},\nu}^{H(L)}$ represent the prefactor and broadened vibrational generation rate of a mode ν, respectively. $\Gamma_{\mathrm{em},\nu}^{H(L)}$ is given by

$$\Gamma_{\mathrm{em},\nu}^{H(L)}(V) = \int_0^\infty W(\omega - \Omega_\nu^{H(L)}, \sigma_{\mathrm{ph},\nu})\ \gamma_{\mathrm{em},\nu}^{H(L)}(V,\omega)\ \mathrm{d}\omega. \tag{6}$$

Here we use a Gaussian distribution function $W(\omega - \Omega_\nu^{H(L)}, \sigma_{\mathrm{ph},\nu}) = \frac{1}{\sigma_{\mathrm{ph},\nu}\sqrt{2\pi}} \exp\left(-\frac{[\omega-\Omega_\nu^{H(L)}]^2}{2\sigma_{\mathrm{ph},\nu}^2}\right)$ characterized by a standard deviation $\sigma_{\mathrm{ph},\nu}$. In Eq. 6, the vibrational emission rate $\gamma_{\mathrm{em},\nu}^{H(L)}$ in the low-temperature limit is given by

$$\gamma_{\mathrm{em},\nu}^{H(L)}(V,\omega) = \lambda_{\mathrm{em},\nu}^{H(L)}\ (eV - \hbar\omega)\ \theta(eV - \hbar\omega), \tag{7}$$

where $\lambda_{\mathrm{em},\nu}^{H(L)}$ is the emission rate constant[3,4,6] and $\theta(eV - \hbar\omega)$ is the Heaviside step function. We combine Eqs. 6 and 7 to the following expression:

$$\Gamma_{\mathrm{em},\nu}^{H(L)}(V) = \frac{\lambda_{\mathrm{em},\nu}^{H(L)}}{\sigma_{\mathrm{ph},\nu}\sqrt{2\pi}} \int_0^{eV/\hbar} (eV - \hbar\omega)\ \exp\left(-\frac{\left[\omega - \Omega_\nu^{H(L)}\right]^2}{2\sigma_{\mathrm{ph},\nu}^2}\right)\ \mathrm{d}\omega. \tag{8}$$

We consider that four vibrational modes contribute to the dI/dV structure: the free O–H stretch mode ν(OH), the H-bonded O–H stretch modes ν(OH-O), and the rotation (bending) mode in the surface normal rot$_z$(OH-O). Two different ν(OH-O) modes are associated with the presence of adjacent NH group; two configurations in Fig. S2d are not equivalent, giving rise to two different modes of H-bonded O–H stretch actuating the flip motion [ν(O$_b$H-O$_a$) and ν(O$_a$H-O$_b$) in Fig. S2d]. The free stretch modes, ν(O$_a$H) and ν(O$_b$H), are not equivalent as well, but we neglect the difference because of their relatively small contribution to the spectral shape. As shown in Fig. S2c, ν(O$_b$H-O$_a$) [ν(O$_a$H-O$_b$)] contributes to $\Gamma_{\mathrm{B}}^{L\to H(H\to L)}$. We assume $\Gamma_{0,\mathrm{B}}^{L} = 1\times10^{-4}$ s^{-1} and $\Gamma_{0,\mathrm{B}}^{H} = 1\times10^{2}$ s^{-1} to reproduce the spectral background. We adopt the DFT values for $\lambda_{\mathrm{em},\nu}^{H(L)}$, $\sigma_{\mathrm{ph},\nu}$, $\Omega_{\mathrm{rot}_z(\mathrm{OH\text{-}O})}^{H(L)}$, and $\Omega_{\nu(\mathrm{OH})}^{H(L)}$, calculated for $(\mathrm{OH})_2$ on Cu(110), and assume $\Omega_{\nu(\mathrm{O}_{b(a)}\mathrm{H\text{-}O}_{a(b)})}^{H} = \Omega_{\nu(\mathrm{O}_{b(a)}\mathrm{H\text{-}O}_{a(b)})}^{L}$, since the difference is expected to be less than 1 meV.[4] Thus, the dI/dV recorded over B is fitted as shown in Fig. S2f, by optimizing the values of $C_{\nu,\mathrm{B}}$, $\Omega_{\nu(\mathrm{O}_b\mathrm{H\text{-}O}_a)}$, and $\Omega_{\nu(\mathrm{O}_a\mathrm{H\text{-}O}_b)}$.

As a result, we obtain the vibrational energies: $\hbar\Omega_{\nu(\mathrm{O}_b\mathrm{H}\text{-}\mathrm{O}_a)}$ = 403±4 meV and $\hbar\Omega_{\nu(\mathrm{O}_a\mathrm{H}\text{-}\mathrm{O}_b)}$ = 428±2 meV. The former (latter) energy is higher (lower) than 414 meV for $(\mathrm{OH})_2$.[3] The difference indicates that H-bond interaction in $\mathrm{O}_b\mathrm{H}\cdots\mathrm{O}_a\mathrm{H}$ is stronger than that in $\mathrm{O}_a\mathrm{H}\cdots\mathrm{O}_b\mathrm{H}$, which is consistent with the observation that the former configuration (Fig. S2a) is more stable than the latter (Fig. S2b). Using the fitting parameters, we reproduce the relative occupation $n_{\mathrm{B}}^{H(L)}$ as shown in Fig. S2e. It indicates that n_{B}^{H} increases (decreases) upon the excitation of $\nu(\mathrm{O}_b\mathrm{H}\text{-}\mathrm{O}_a)$ [$\nu(\mathrm{O}_a\mathrm{H}\text{-}\mathrm{O}_b)$], which causes the peak (dip) structure in the dI/dV recorded over B.

Figure S2f also shows dI/dV curves recorded over different positions (A and C in Fig. S2a). In a similar way, $\nu(\mathrm{O}_b\mathrm{H}\text{-}\mathrm{O}_a)$ [$\nu(\mathrm{O}_a\mathrm{H}\text{-}\mathrm{O}_b)$] is responsible for the dip (peak) structure in the dI/dV recorded over A. In contrast, the dI/dV recorded over C has no structure, indicating that $\mathrm{NH}\cdots\mathrm{OH}$ is fixed in the orientation.

References

1 T. Kumagai, M. Kaizu, H. Okuyama, S. Hatta, T. Aruga, I. Hamada and Y. Morikawa, *Phys. Rev. B*, 2009, **79**, 035423.

2 A. Shiotari, Y. Kitaguchi, H. Okuyama, S. Hatta and T. Aruga, *Phys. Rev. Lett.*, 2011, **106**, 156104.

3 Y. Ootsuka, T. Frederiksen, H. Ueba and M. Paulsson, *Phys. Rev. B*, 2011, **84**, 193403.

4 H. Okuyama, A. Shiotari, T. Kumagai, S. Hatta, T. Aruga, Y. Ootsuka, M. Paulsson and H. Ueba, *Phys. Rev. B*, 2012, **85**, 205424.

5 I. Hamada, T. Kumagai, A. Shiotari, H. Okuyama, S. Hatta and T. Aruga, *Phys. Rev. B*, 2012, **86**, 075432.

6 T. Frederiksen, M. Paulsson, M. Brandbyge and A.-P. Jauho, *Phys. Rev. B*, 2007, **75**, 205413.

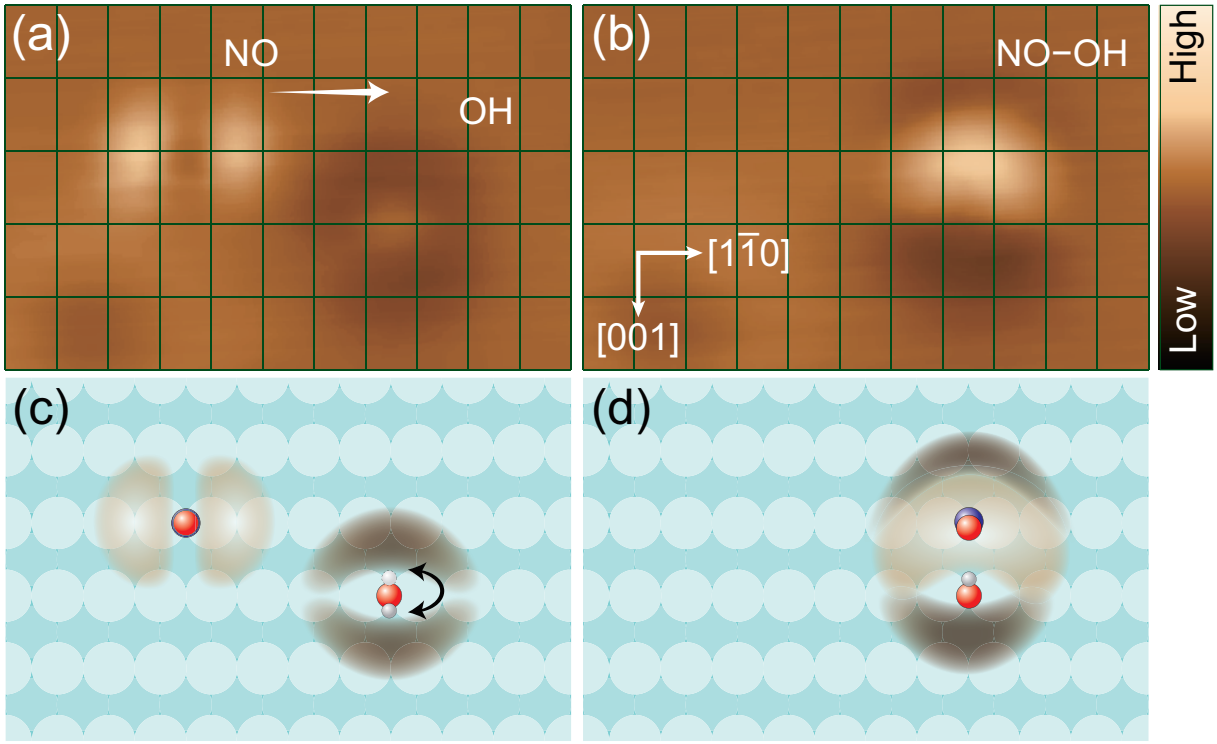

Fig. S1: (a) STM images of NO and H_2O molecules. The two molecules locate on the neighboring two Cu rows (V = 30 mV, I = 0.5 nA: hereinafter the same shall apply). (b) STM image of a NO–water complex, after manipulating H_2O like as an arrow in (a). The image size in (a) and (b) is 28 × 18 Å^2. (c) and (d) Schematic illustrations of the STM shape and molecular configration of (a) and (b), respectively. White, red, and blue sphere denote H, O, and N atom, respectively.

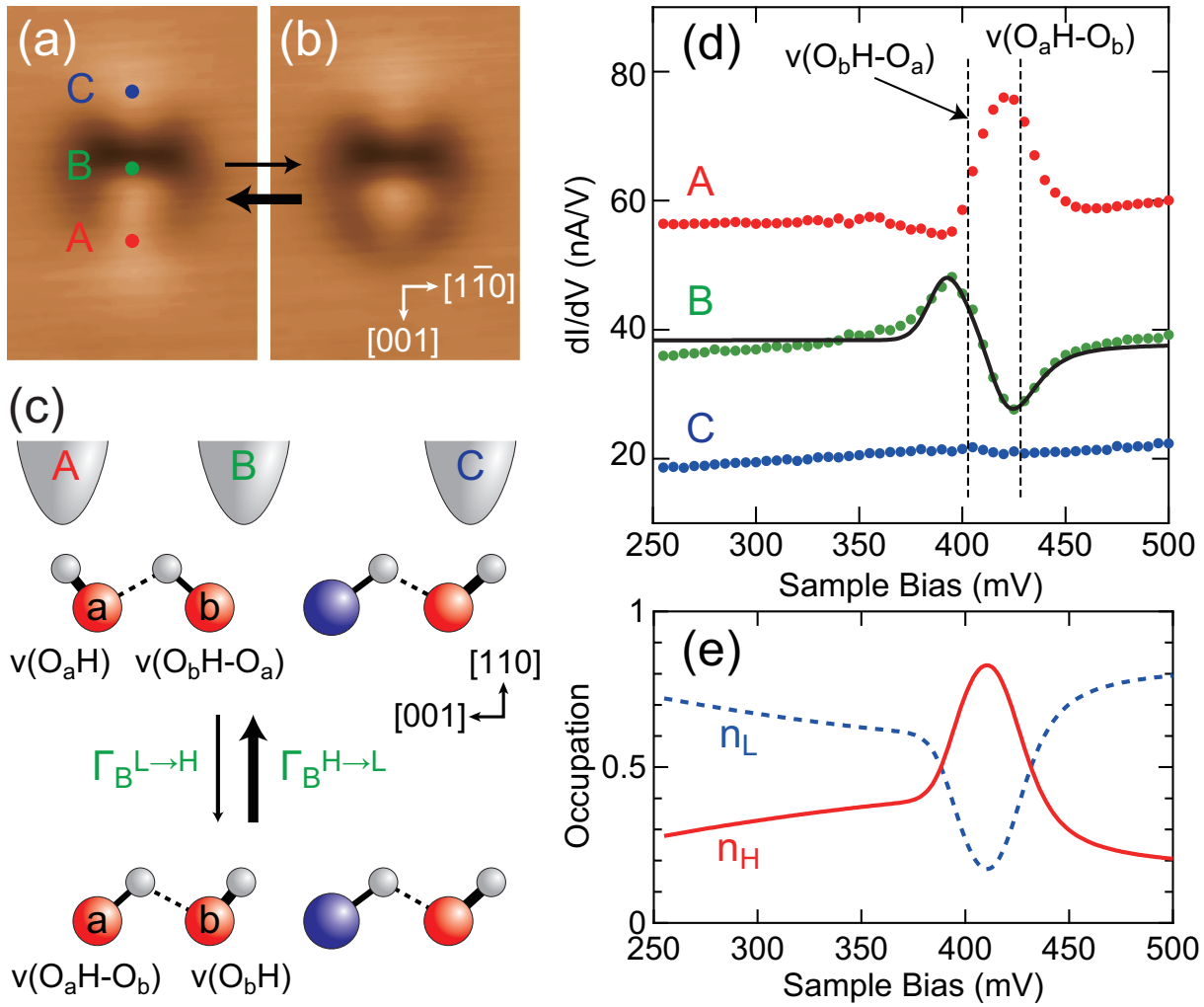

Fig. S2: (a) STM image of a $(OH)_2\cdots$NH–OH product. (b) An image after applying a voltage pulse of 250 mV. This image was turned back to the image of (a) spontaneously at V = 30 mV. The image size in (a) and (b) is 18 × 25 Å^2. (c) Schematic illustration of the flipping motion of the complex. STM tips labeled A–C correspond to the position A–C in (a). White, red, and blue sphere denote H, O, and N atoms, respectively. O_a and O_b denote oxygen atoms which are originated from the first H_2O and the NO molecule, respectively. The configuration in the top (bottom) corresponds to that in (a) [(b)]. (d) dI/dV spectrum recorded over positions A–C in (a). Spectra over the position A and B are vertically offset for clarity. The peak-and-dip features are ascribed to the H-bonded O–H stretch modes: ν(O$_b$H-O$_a$) and ν(O$_a$H-O$_b$). The solid curve in B shows the fitting result, which yields the vibrational energy of ν(O$_b$H-O$_a$) [ν(O$_a$H-O$_b$)] at 403 meV (428 meV). (e) The voltage dependence of the relative occupation $n_{L(H)}$ over B deduced from the fitting. $n_{L(H)}$ represents the occupation of the low- (high-) conductance states over B, corresponding to the configurations in (a) [(b)].